

Giant quantized plateau in the THz Faraday angle in gated Bi₂Se₃

Gregory S. Jenkins,^{1,2,*} Andrei B. Sushkov,^{1,2,3} Don C. Schmadel,^{1,2} M.-H. Kim,^{1,2}

Matthew Brahlek,⁴ Namrata Bansal,⁴ Seongshik Oh,⁴ and H. Dennis Drew^{1,2,3}

¹*Department of Physics, University of Maryland at College park, College Park, Maryland, 20742, USA*

²*Center for Nanophysics and Advanced Materials,*

University of Maryland at College park, College Park, Maryland, 20742, USA

³*Materials Research Science and Engineering Center,*

University of Maryland at College park, College Park, Maryland, 20742, USA

⁴*Department of Physics and Astronomy, The State University of New Jersey, Piscataway, New Jersey 08854, USA*

(Dated: September 7, 2012)

We report gated terahertz Faraday angle measurements on epitaxial Bi₂Se₃ thin films capped with In₂Se₃. A plateau is observed in the real part of the Faraday angle at an onset gate voltage corresponding to no band bending at the surface which persists into accumulation. The plateau is two orders of magnitude flatter than the step size expected from a single Landau Level, quantized in units of the fine structure constant. At 8 T, the plateau extends over a range of gate voltage that spans an electron density greater than 14 times the quantum flux density. Both the imaginary part of the Faraday angle and transmission measurements indicate dissipative off-axis and longitudinal conductivity channels associated with the plateau.

In two-dimensional quantum Hall systems, one-dimensional edge states are topologically protected quantum states characterized by integer Chern numbers. Three dimensional topological insulators are characterized by a quantized magneto-electric term appearing in the effective Lagrangian, quantized in units of the fine structure constant $\alpha = \frac{e^2}{hc}$.¹⁻⁵ The quantization condition of this magneto-electric term stems from a Chern-Simons form of the Berry phase, known as the axion angle in particle physics.^{6,7} In the non-trivial case, the axion angle attains odd-multiple values of π resulting in two dimensional topologically protected surface states that are spin polarized. By breaking time reversal symmetry, these singly-occupied two dimensional Dirac states are predicted to exhibit a 1/2-quantized Hall step near the Dirac point, a smoking gun signature of the topological origin of the surface state.⁷ Kerr or Faraday terahertz (THz) measurements offer a method to cleanly measure this quantized step since no contacts to the sample are required alleviating complications that can occur from gating a sample with no edges.^{8,9}

Bi₂Se₃ has a single surface-state Dirac cone whose Dirac point is well above the valence band. The material has one of the largest bulk band gaps of all known topological insulators allowing access to the Dirac cone over a large range of Fermi energies. However, Bi₂Se₃ is susceptible to n-type bulk doping from defects as well as environmental surface doping.⁹⁻¹⁵ High quality epitaxially grown thin films of Bi₂Se₃ have relatively low n-type bulk doping,¹⁶ and subsequent capping with In₂Se₃ further lowers the Fermi level of the surface states allowing conventional gating to reach the Dirac point.⁸

No previous optical probe has been reported that attempts to measure the quantized Hall effect on a topological insulator as a function of gate voltage.^{8,9,17-22} We report Faraday angle and transmission measurements performed at a fixed laser frequency of $\omega/2\pi = 0.74$ THz as a function of gate voltage at discrete magnetic fields up

to 8 T on two topological insulating films. These Bi₂Se₃ thin films, 40 and 60 quintuple layers thick, were grown epitaxially onto 0.5 mm thick sapphire substrates and capped with 10 nm thick In₂Se₃ layers without breaking vacuum.^{16,23} As depicted in Figure 1(a), the dielectric Parylene-C was deposited encasing the sample to a thickness of 590 nm (620 nm) for the 60 (40) QL film. A NiCr top gate and a NiCr antireflection coating were evaporated onto the Parylene-C. For the 60 QL device, the gate moves a charge density of $2.6 \times 10^{10} e/\text{cm}^2$ per volt on or off the Bi₂Se₃ film.

The Faraday angle is related to the off-axis conductivity σ_{xy} of a thin film by $\theta_F \approx Z\sigma_{xy}/(1 + Z\sigma_{xx})$ where $Z = Z_0/(n_s + 1)$, and n_s is the substrate index of refraction, Z_0 is the impedance of free space, and σ_{xx} is the longitudinal conductivity.^{8,24} Considering the case where the cyclotron frequency ω_c is large compared to the scattering rate γ and radiation frequency ω , and $Z\sigma_{xx}$ is small compared with 1, crossing a Landau level results in $\Delta\theta_F \approx 2\alpha/(n_s + 1)$. Under very specific geometric conditions, the substrate properties can be ignored and $\Delta\theta_F$ is quantized exactly in units of α .^{1,4,5,25} More generally, the quantization of $\Delta\theta_F$ from step-to-step is scaled by the material properties of the substrate and any longitudinal conductivity contributions (like a conducting gate or other dissipation channels), as well as corrections from non-zero γ and ω .

The complex Faraday angle measurement at THz frequencies utilizes polarization-modulated fixed-frequency laser radiation, a technique detailed elsewhere.²⁴ The beam is normally incident on the film held at 10 K that is maintained in a normally applied magnetic field. The transmission through the film is measured concurrently. The differential Faraday angle $\Delta\theta_F$ and the differential transmission ΔT are differences between the optical signals measured at a fixed gate voltage $V_g^0 = +170$ V and the signals measured at a variable gate voltage V_g .

The differential Faraday angle $\Delta\theta_F$ and differential

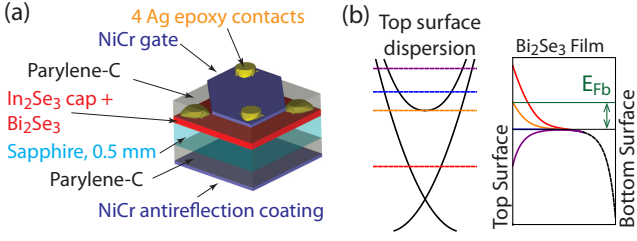


FIG. 1: **Sample layout and band bending diagram:** (a) A Bi₂Se₃ 60 (40) QL film is capped with 10 nm of In₂Se₃, and encased in 590 nm (620 nm) of Parylene-C. A NiCr gate $\sim 400 \Omega/\square$ and antireflection coating $\sim 275 \Omega/\square$ were deposited by evaporation. Pairs of silver epoxy contacts were made to the Bi₂Se₃ film and NiCr gate. (b) A band bending diagram showing the conduction band edge from large negative gate voltages (red) to large positive gate voltages (purple), depicted in both the topological surface state dispersion and a cross-section of the film. The specific Fermi levels at the surface depicted in blue and orange are referenced in the text as the flat band (FB) and conduction band edge (CBE) conditions, respectively.

transmission ΔT as a function of gate voltage at fixed fields for the two devices are reported in Figure 2. Measurements performed at THz frequencies on the same 60 quintuple layer (QL) device, but as a function of magnetic field, are reported in reference 8. The gate sweeps at fixed magnetic field presented here offer better signal-to-noise than previous measurements. $Re(\Delta\theta_F)$ is measured to within a standard deviation of the mean of $30 \mu\text{rad}$ without systematic drift effects associated with changing the magnetic field. With this additional sensitivity, $Re(\Delta\theta_F)$ of the 60 QL film shows an extraordinarily flat response over a tremendous span of gate voltages, from +170 V to +70 V.

The previous THz measurements on the 60 QL film provide an overview of the characteristics of the film. The salient features of the THz data were captured utilizing two gate dependent Drude terms in the conductivity: the first term was primarily associated with the bulk carriers of the screened region near the top surface (IB), and the second term represented the top topological surface state (TSS). The conception of the model was based upon the Thomas-Fermi band bending in the film, depicted in Figure 1(b). All carrier contributions in the film were found to be n-type. Based upon the small measured cyclotron mass $m_c = \hbar k_F/v_F$ at high negative gate voltages, the Dirac point was estimated to be in the vicinity of -180 V. A 70 meV shift of the Dirac point toward the conduction band edge (relative to the characterized vacuum interface)^{26–28} due to the Bi₂Se₃/In₂Se₃ interface was deduced from the functional form of the scattering rate.^{8,29,30} In Figure 2, the conduction band edge (CBE) and flat band (FB), the gate voltage at which no band bending occurs on the top surface, are demarcated in the graphs by green and gray vertical dashed lines.

There are a number of important observations associ-

ated with the plateau in the $Re(\Delta\theta_F)$ shown in Figure 2(a) and (g). The first is the degree of flatness. Such an extremely flat response is very difficult to reproduce invoking non-quantized behavior. In the simplest view, a gate moves electrons to the film with increasingly positive gate voltage, predictably lowering the transmission as reported in Figure 2(c), yet the real part of the Faraday angle remains constant over a large range of voltages.

A slightly more sophisticated approach using the same multi-fluid Drude model that reproduced the features of all the data reported in reference 8 does not reproduce the extremely flat behavior of the $Re(\Delta\theta_F)$ gate sweeps in fixed magnetic field, as shown in Figure 2(i). The gate dependent scattering rates of the TSS and IB Drude terms give rise to an extremum in the modelled response of Figure 2(i). The observation in Figure 2(g) of such a flat response over such a large range of gate voltages is irreconcilable with two gate-dependent n-type Drude terms while maintaining consistency with previous optical data. The data suggests the existence of localized states associated with σ_{xy} which absorb the transferred charge from the gate but give no additional contribution to $Re(\theta_F)$.

The formation of Landau levels is one way that can provide localized states. Although we currently do not have a complete explanation for the observed plateau, recent dc Hall measurements on highly doped $\gtrsim 10^{19} \text{ cm}^{-3}$ Bi₂Se₃ bulk crystals, performed on many different samples spanning four orders of magnitude in thickness, appear to support the scenario that an extraordinary bulk quantum Hall effect (QHE) occurs in which each pair of QLs contribute a distinct Landau Level to the Hall response.³¹ These Landau levels appear to act in unison such that the step-to-step height $\Delta\sigma_{xy} = (\# \text{ of QLs}) \frac{e^2}{h}$. However, ρ_{xx} oscillates but does not go to zero, remaining comparable with ρ_{xy} even within plateaus, indicating appreciable dissipation. Within this context, we discuss the character of the observed plateau in the $Re(\Delta\theta_F)$ shown in Figure 2(g).

For small longitudinal conductivity ($Z\sigma_{xx} \ll 1$) and large cyclotron frequency $\omega_c \gg \gamma, \omega$, the finite-frequency off-axis conductivity $\sigma_{xy} = \Omega_0\omega_c/((\gamma - i\omega)^2 + \omega_c^2)$ reduces to $\sigma_{xy} = ne/B$ since the spectral weight $\Omega_0 = ne^2/m$ and the cyclotron frequency $\omega_c = eB/m_c$. The electron density n changes by $B/(h/e)$ when the Fermi level sweeps through a single Landau Level at fixed magnetic field B , so $Z_0\Delta\sigma_{xy} = 2\alpha$. Since sapphire has an index of refraction of $n \approx 3$, $Z_0/R \approx 1$ for the NiCr gate, and $Z_0\sigma_{xx} \approx 1$, the change in Faraday angle upon stepping through a Landau Level is expected to be $\Delta\theta_F \approx \alpha/3 = 2.4 \text{ mrad}$. The $Re(\Delta\theta_F)$ is flat over a range of at least 100 V to within 1/80 of the expected quantum step size from a single Landau level.

The plateau at positive gate voltage decreases in width with decreasing magnetic field qualitatively consistent with Landau level behavior. The plateau appears at surface Fermi levels at the flat band condition, and persists into accumulation. At negative gate voltages where the

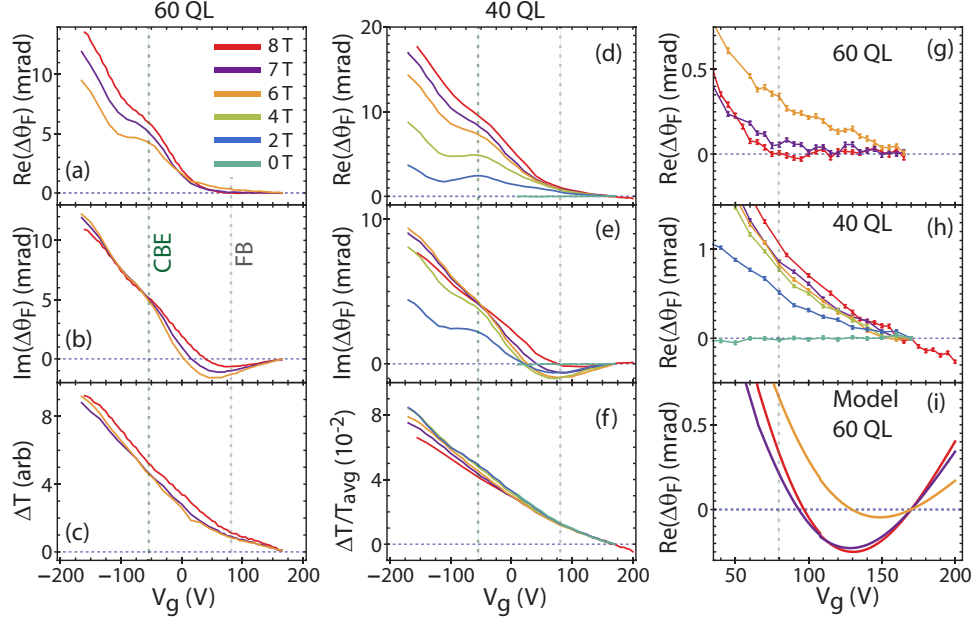


FIG. 2: $\Delta\theta_F$ and ΔT data and model: All transmission and Faraday angle measurements were performed at $\omega/2\pi = 0.74$ THz at discrete magnetic fields that are color coded according to the key in panel (a). Differential optical measurements are differences between two different gate voltages, one is fixed at $V_g^0 = 170$ V and the other V_g is variable. The differential transmission ΔT is normalized to the average transmission T_{avg} of the two gate values only in panel (f). Flat band (FB) and the conduction band edge (CBE) conditions at the surface are demarcated with dotted lines in all figures, which take into account a 70 meV shift toward mid-gap of the interface state. (a-c) Differential measurements of the Faraday angle and transmission are shown for the 60 QL film maintained at 10 K and (d-f) the 40 QL film maintained at 10 K. (g,h) A zoomed view of the $\text{Re}(\Delta\theta_F)$ for the 60 and 40 QL films, respectively. (i) A model of the $\text{Re}(\Delta\theta_F)$ for the 60 QL device incorporating the Drude parameters that reproduce all the optical data in reference 8.

surface Fermi level is below the conduction band edge, the step-like feature at -70 V is attributed to a sudden drop in scattering rate as the surface state decouples from the bulk carriers.⁸ This feature does not display the expected behavior by a quantized Hall step upon changing the magnetic field.

The width of the positive-voltage plateau is much larger than expected from a single Landau level. The gate moves $2.6 \times 10^{12} e/\text{cm}^2$ over 100 V, and each Landau level is occupied by an electron density of $B/(h/e) = 1.9 \times 10^{11} \text{ cm}^{-2}$ in 8 T. At least 14 Landau levels are traversed over the span of the plateau.

Given that no Landau level steps are discernable in the data at negative gate voltages, and the topological surface state is singly occupied contributing at most 1 Landau level of charge, the conclusion is that the plateau must primarily be a bulk effect.

Figure 2(d-f) and (h) show gated THz measurements performed on the 40 QL Bi_2Se_3 film. Although the qualitative behavior is very similar to the 60 QL film, there are no plateaus in the $\text{Re}(\Delta\theta_F)$ response. The Thomas-Fermi screening length is estimated to be about 14 nm based upon dc measurements of bulk densities of similarly prepared films performed over a wide range of thicknesses.^{8,16} Gating the top surface of the 40 nm film will affect the accumulated bottom surface layer much

more than the thicker 60 nm film. An additional gate dependent conductivity channel associated with the bottom surface accumulation layer can give rise to a different behavior. Study of thicker films is necessary to verify this thickness effect.

The gate dependence of ΔT and $\text{Im}(\Delta\theta_F)$ of the 60 QL film over the same voltage range where the plateau exists indicates dissipation in the σ_{xx} and σ_{xy} channels. In this regard, the similarities between the reported dc measured bulk QHE and the gated THz measurements are striking. The dc data show plateaus in the Hall conductivity, consistent with the sum of many Landau level contributions, in the presence of significant dissipative channels.

However, even the highest positive applied gate voltage of $+170$ V, which causes the conduction band to bend downward at the surface as depicted in Figure 1(b), only results in a Fermi level of 45 meV above the conduction band edge at the surface. This Fermi level translates into a bulk density of $\sim 3 \times 10^{18} \text{ cm}^{-3}$, about an order of magnitude less than the dc measurements on bulk crystals reporting bulk QHE.³¹

More important, the most significant difference between the THz and dc experiments is associated with the gradient of the potential from band bending effects in the film produced by the applied gate. In the case of the

dc measurements, identical independent two-dimensional layers exhibiting the QHE are known to summate in the expected way, corresponding to a single Landau level but with a degeneracy corresponding to the number of layers.³² However, if the potential varies appreciably from layer to layer, the Landau levels would not remain degenerate nor give well defined large steps. In our case, screening effects are expected to cause such a misalignment of Landau levels. At +170 V, the bands are bent downward by ~ 30 meV over ~ 14 QL (the screening length), producing ~ 2 meV change in potential energy from QL to QL. The Landau level spacing (cyclotron frequency) in 8 T is only ~ 4 meV, so one might expect the variation of potential would wipe out any additive effect from independent Landau levels that could produce a wide Hall plateau.

This may indicate that the contributing Landau levels are not independent, but interact in a way that tends to lock the levels together. For the dc measured bulk QHE of reference 31, the scenario put forth was that the quintuple layers of Bi₂Se₃ decouple, forming independent 2-DEGs. Many questions remain about the nature of this

decoupling since Shubnikov-de Haas measurements show a 3-D Fermi surface.^{33,34} It is also puzzling how the QHE survives the large measured σ_{xx} in the Hall plateaus.³¹ Similarly in this paper we report the phenomenology of an extremely flat Hall response observed at sub-THz frequencies, manifesting in the real part of the Faraday angle that is flat to within 1/80 of the expected quantization step size for a single Landau level. This plateau extends over a large range of gate induced carrier density change of $\sim 3 \times 10^{12} e/cm^2$, occurring above the conduction band edge, corresponding to more than 14 occupied Landau levels. A full understanding of this plateau is likely tied to understanding the bulk QHE, which currently remains elusive.

The authors thank M. S. Fuhrer, T. D. Stanescu, and S. Das Sarma for helpful conversations. The work at the University of Maryland is supported by NSF (DMR-1104343) and CNAM. The Rutgers work is supported by IAMDN of Rutgers University, National Science Foundation (NSF DMR-0845464,) and Office of Naval Research (ONR N000140910749).

-
- * URL: <http://www.irhall.umd.edu>; Electronic address: GregJenkins@MyFastMail.com
- ¹ Volkov, V. A. & Mikhailov, S. A. Quantization of the Faraday effect in systems with a quantum Hall effect. *JETP Letters* **41**, 389 (1985).
 - ² Hasan, M. Z. & Kane, C. L. Colloquium: Topological insulators. *Reviews of Modern Physics* **82**, 3045–3067 (2010).
 - ³ Qi, X.-L. & Zhang, S.-C. Topological insulators and superconductors. *Reviews of Modern Physics* **83**, 1057–1110 (2011).
 - ⁴ Maciejko, J., Qi, X.-L., Drew, H. D. & Zhang, S.-C. Topological quantization in units of the fine structure constant. *Physical Review Letters* **105**, 166803 (2010).
 - ⁵ Tse, W.-K. & MacDonald, A. H. Giant magneto-optical kerr effect and universal faraday effect in thin-film topological insulators. *Physical Review Letters* **105**, 057401 (2010).
 - ⁶ Wilczek, F. Two applications of axion electrodynamics. *Physical Review Letters* **58**, 1799–1802 (1987). URL <http://link.aps.org/doi/10.1103/PhysRevLett.58.1799>.
 - ⁷ Qi, X.-L., Hughes, T. L. & Zhang, S.-C. Topological field theory of time-reversal invariant insulators. *Physical Review B* **78**, 195424 (2008).
 - ⁸ Jenkins, G. S. *et al.* High mobility topological interface state probed by terahertz measurements. *arXiv:1208.3881* (2012). URL <http://arxiv.org/abs/1208.3881>.
 - ⁹ Jenkins, G. S. *et al.* Terahertz kerr and reflectivity measurements on the topological insulator Bi₂Se₃. *Physical Review B* **82**, 125120 (2010).
 - ¹⁰ Butch, N. P. *et al.* Strong surface scattering in ultrahigh-mobility Bi₂Se₃ topological insulator crystals. *Physical Review B* **81**, 241301 (2010).
 - ¹¹ Kong, D. *et al.* Rapid surface oxidation as a source of surface degradation factor for Bi₂Se₃. *ACS Nano* **5**, 4698–4703 (2011).
 - ¹² Checkelsky, J. G., Hor, Y. S., Cava, R. J. & Ong, N. P. Bulk band gap and surface state conduction observed in voltage-tuned crystals of the topological insulator BiSe. *Physical Review Letters* **106**, 196801 (2011).
 - ¹³ Analytis, J. G. *et al.* Two-dimensional surface state in the quantum limit of a topological insulator. *Nature Physics* **6**, 960–964 (2010).
 - ¹⁴ Steinberg, H., Gardner, D. R., Lee, Y. S. & Jarillo-Herrero, P. Surface state transport and ambipolar electric field effect in Bi₂Se₃ nanodevices. *Nano Letters* **10**, 5032–5036 (2010).
 - ¹⁵ Kim, D. *et al.* Surface conduction of topological dirac electrons in bulk insulating Bi₂Se₃. *Nature Physics* **8**, 460–464 (2012).
 - ¹⁶ Bansal, N., Kim, Y. S., Brahlek, M., Edrey, E. & Oh, S. Thickness-independent surface transport channel in topological insulator Bi₂Se₃ thin films. *arXiv:1104.5709* (2011).
 - ¹⁷ Sushkov, A. B. *et al.* Far-infrared cyclotron resonance and faraday effect in Bi₂Se₃. *Physical Review B* **82**, 125110 (2010).
 - ¹⁸ Brune, C. *et al.* Quantum hall effect from the topological surface states of strained bulk hgte. *Physical Review Letters* **106**, 126803 (2011).
 - ¹⁹ Hancock, J. N. *et al.* Surface state charge dynamics of a high-mobility three dimensional topological insulator. *1105.0884* (2011). URL <http://arxiv.org/abs/1105.0884>.
 - ²⁰ Kvon, Z. *et al.* Cyclotron resonance of dirac fermions in hgte quantum wells. *JETP Letters* **94**, 816819 (2012).
 - ²¹ Schafgans, A. A. *et al.* Landau level spectroscopy of surface states in the topological insulator bi_{0.91}sb_{0.09} via magneto-optics. *Physical Review B* **85**, 195440 (2012).
 - ²² Valdes Aguilar, R. *et al.* Terahertz response and colossal kerr rotation from the surface states of the topological in-

- insulator Bi_2Se_3 . *Physical Review Letters* **108**, 087403 (2012).
- ²³ Bansal, N. *et al.* Epitaxial growth of topological insulator Bi_2Se_3 film on Si(111) with atomically sharp interface. *Thin Solid Films* **520**, 224–229 (2011).
 - ²⁴ Jenkins, G. S., Schmadel, D. C. & Drew, H. D. Simultaneous measurement of circular dichroism and faraday rotation at terahertz frequencies utilizing electric field sensitive detection via polarization modulation. *Review of Scientific Instruments* **81**, 083903 (2010).
 - ²⁵ O’Connell, R. F. & Wallace, G. Ellipticity and faraday rotation due to a two-dimensional electron gas in a metal-oxide-semiconductor system. *Physical Review B* **26**, 2231–2234 (1982).
 - ²⁶ Xia, Y. *et al.* Observation of a large-gap topological-insulator class with a single dirac cone on the surface. *Nature Physics* **5**, 398–402 (2009).
 - ²⁷ Zhu, Z.-H. *et al.* Rashba spin-splitting control at the surface of the topological insulator Bi_2Se_3 . *Physical Review Letters* **107**, 186405 (2011).
 - ²⁸ Bahramy, M. S. *et al.* Emergent quantum confinement at topological insulator surfaces. *arXiv:1206.0564* (2012). URL <http://arxiv.org/abs/1206.0564>.
 - ²⁹ Korenman, V. & Drew, H. D. Subbands in the gap in inverted-band semiconductor quantum wells. *Physical Review B* **35**, 6446–6449 (1987).
 - ³⁰ Agassi, D. & Korenman, V. Interface states in band-inverted semiconductor heterojunctions. *Physical Review B* **37**, 10095–10106 (1988).
 - ³¹ Cao, H. *et al.* Quantized hall effect and shubnikov-de haas oscillations in highly doped Bi_2Se_3 : Evidence for layered transport of bulk carriers. *Physical Review Letters* **108**, 216803 (2012).
 - ³² Haavasoja, T. *et al.* Magnetization measurements on a two-dimensional electron system. *Surface Science* **142**, 294297 (1984).
 - ³³ Kohler, H. Conduction band parameters of Bi_2Se_3 from Shubnikov-de Haas investigations. *physica status solidi (b)* **58**, 91100 (1973).
 - ³⁴ Eto, K., Ren, Z., Taskin, A. A., Segawa, K. & Ando, Y. Angular-dependent oscillations of the magnetoresistance in Bi_2Se_3 due to the three-dimensional bulk fermi surface. *Physical Review B* **81**, 195309 (2010).